© Universiti Tun Hussein Onn Malaysia Publisher's Office

IJIE

http://penerbit.uthm.edu.my/ojs/index.php/ijie
ISSN : 2229-838X e-ISSN : 2600-7916

The International Journal of Integrated Engineering

Multibeam Array Antenna with Compact Size Butler Matrix for Millimeter-Wave Application

Noorlindawaty Md Jizat[1*], Yoshihide Yamada[2], Zubaida Yusoff [1]

[1]Faculty of Engineering,
Multimedia University, Cyberjaya, 62300, MALAYSIA

[2]Communication Systems and Network (CSN i-Kohza) MJIIT,
Universiti Teknologi Malaysia Kuala Lumpur, 54100, MALAYSIA

*Corresponding Author

DOI: https://doi.org/10.30880/ijie.2023.15.03.014
Received 06 November 2022; Accepted 18 April 2023; Available online 15 August 2023

Abstract: New radio wave technologies of millimeter-wave (mmWave), compact cell size, and multi beam base station are introduced with the recent development of the 5G mobile system. The Butler Matrix (BM) feed circuit is the most preferable candidate for the 5G mobile system since it can achieve multi beam radiation patterns at the array antenna, provide structural compactness and produce good multi beams. The BM circuit is typically built on a single dielectric substrate. However, in this single-substrate structure, the micro strip line connecting several circuit elements in the BM spans over a large area, resulting in significant feeding loss in the millimeter frequency band. In this study, a compact size circuit configuration of BM is proposed, where the original single-substrate structure is modified into a two-substrate stacking structure. The via-hole is designed to connect the two substrates with minimal path loss. The BM is built for the 28 GHz band with four inputs and four outputs. The phase delay is optimized using via-hole to produce the phase difference of ±45º and ±135º. The coupling for the hybrid is -3 dB, while the transmission coefficient of -6 ± 3 is achieved from the BM structure and, the return loss (S_{ii}) for both input and output ports are less than -10 dB. The two-substrate BM is combined with the rectangular patch antenna and the via-hole patch antenna in a planar configuration of 0.5 λ_0 spacing to obtain the radiation patterns. When the Port 1 through Port 4 of the BM are fed, four beams are created, with peak gains of 11.2 dBi, 9.87 dBi, 10.2 dBi, and 11.7 dBi, respectively, towards +16°, -35°, +39°, and -12°. The analysis includes the radiation performance from the ideal value and from the BM input. Three-dimensional representations of good multibeam radiation patterns are obtained after each input signal of the BM is fed.

Keywords: Via-hole, millimeter-wave, Butler Matrix, beam forming

1. Introduction

Fifth-generation mobile system (5G) networks are designed to ease the current infrastructure's burden by providing much faster speeds rates via improved channel bandwidths [1-2]. Inter-cell interference is a major challenge in dense networks that need to be eliminated or minimized. To overcome the inter-cell limitation, millimeter wave's (mmWave's) at higher frequency bands enable for more capacity. However, in terms of propagation properties, mmWave systems have much higher total losses than microwave systems. The target signal quality is improved while interference is minimized by employing beam formation using antenna arrays. Antenna array beamforming is essential for mmWave systems since the antenna arrays are anticipated to be used at both communication link ends to compensate for the increased free space route loss in the first meter of transmission [3].

Antenna beam forming plays a significant role in establishing and maintaining a robust communication link. One of the most commonly beamforming used is Butler Matrix (BM) due to low cost, simple structure and planar. However, due

*Corresponding author: noorlindawaty.jizat@mmu.edu.my

to the high path and penetration losses at millimeter wavelengths, the antenna performance deteriorates. For mmWave beamforming, previous work has used finline technique, hollow waveguide, switches in single planar, substrate integrated waveguides (SIW), and tri-layer configurations [4-9]. In [10], by eliminating the 0 dB crossover, a planar BM is presented, and a modified BM without the phase shifter component is shown in [11], allowing for greater frequency range phase shift stability while minimising the length and component loss. To reduce mutual coupling, a broadband phase shifter is modified in [12]. When the passive feeding network includes *N* inputs and *N* outputs, where *N* is the power of 2 ($N = 2^n$) made the structure is complex and some of the BM sizes proposed by earlier studies are impractical when a larger matrix is required [13]. BM technology has been widely regarded as a promising alternative for 5G systems, although there is still a gap between the antenna integration of mmWave prototypes and beamforming systems. There are a lot of challenges due to the significant path and penetration losses at mmWave, when the antenna performance suffers due to losses from the BM structure.

In this work, the design of BM structure using the vias is used to reduce the path loss and to provide a compact size. The dual-layer substrate is connected to the BM through circular slot, which is designed at the ground layer which is at the centre of the two substrates. The via pin is used to adjust the amplitude and the phase delay during transition. Patch antenna array is used as the radiating element of the BM structure. Given that the crossover is avoided, this structure is efficient. The via-slot hole's diameter and via pin diameter are used to control the coupling and phase transition of the signal, allowing the BM to minimize amplitude and phase imbalances. For the actual application at 28 GHz with constrained space, the two-substrate configuration's compact design makes the BM size ideal. When the signal is sent from Port 1 to Port 4, the BM creates four beams with peak gains of 11.2 dBi, 9.87 dBi, 10.2 dBi, and 11.7 dBi, correspondingly, directed at +16°, -35°, +39°, and -12°. An antenna electromagnetic simulation, Computer Simulation Technology (CST) is used to analyze the performance of the BM and the multi-beam radiation patterns.

2. Butler Matrix Design

In the conventional BM design, four hybrids, phase shifters and crossovers are arranged in a planar configuration. However, in this technique, two-substrate is used to provide compact size, and via-hole is used to compensate the insertion loss and the phase with minimal loss and produce good multi beams.

2.1 Butler Matrix

As depicted in Fig. 1, a 4x4 BM structure has four hybrids, two 45° phase shifters and two crossovers. When the input port of the BM is given the signal and the BM is integrated to the antenna array, four different beams are formed. The BM network has N ports with N inputs and outputs. A BM can also be used to point the beam by providing a signal to each input port and adjusting the phase across the output ports progressively. According to Moody's design concept, the phase difference between radiating elements for a BM with N elements and for the direction beam point is given by Equation 1 [14]. Phase differences at the output ports are ±45 degrees and ±135 degrees, respectively, for the p^{th} beam angle:

$$\phi_p = \pm \frac{2p-1}{N} \times 180^\circ \tag{1}$$

where $N = 4$, $n = 2$ and $p = 1, 2, \ldots. (n + 1)$.

Thus, by applying the above equation for 4x4 BM, the phase difference is ± 45° for port 1and port 4, while ± 135° for port 2 and port 3, respectively. In a two-substrate via-hole design, the top and bottom layer configurations are connected using the via pin as shown in Fig. 2. The side size is minimized to half of the normal structure when the configuration is used. The BM consists of two passive hybrids on the upper and lower layers, with 45° phase shifters attached by a via pin with a circular hole at the center ground. The use of a crossover connection is removed in these designs, resulting in a significant reduction in the size of the BM and a reduction in losses. Table 1 shows the output phase difference for each of the input ports.

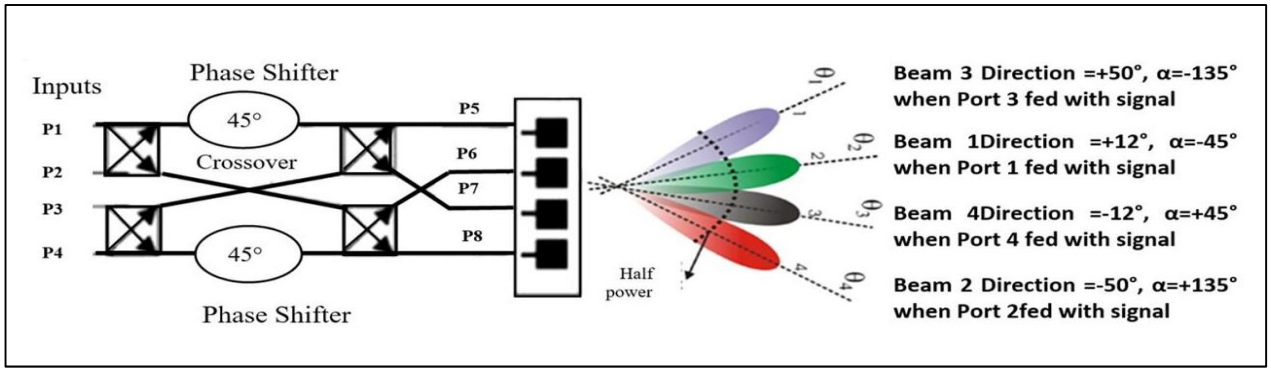

Fig. 1 - 4×4 Butler Matrix phasor excitation with respects

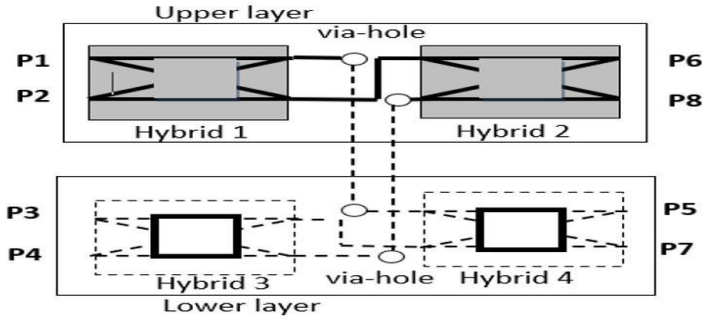

Fig. 2 - Dual-layer Butler Matrix with via-hole structure

Table 1 - Output phases of Butler Matrix

	Output Port 1, P5	Output Port 2, P6	Output Port 3, P7	Output Port 4, P8	Phase Difference
Input Port 1, P1	0	-45	-90	-135	-45
Input Port 2, P2	0	+135	+270	+405	+135
Input Port 3, P3	0	-135	-270	-405	-135
Input Port 4, P4	0	45	90	135	45

2.2 Via-Hole

By adjusting the parameters of the ground circular slot diameter, D_S, microstrip via-hole pin diameter, D_P and the substrate thickness, D_T, the via-hole produces a minimal loss coupling at high frequencies. When connecting the dual-layer substrates as indicated in Fig. 3 (a), the via pin is more flexible, and Fig. 3 (b) shows the surface current flowing via the circular slot through hole. The strip line width, w and length, l is 0.7826 mm and 4 mm. Fig. 4 illustrates an analysis of the effects of various circular slot diameters, via-hole pin diameters, and substrate thicknesses on insertion loss, with the lowest insertion loss occurring at D_S, is 1.2 mm, D_P, is 0.3 mm, and D_T, is 0.254 mm, respectively. The design has input ports (Port 1) on the top layer, while the other port (Port 2) is designed on the lower layer. A path for an electrical signal to travel through is provided by the via-hole, which connects the top and bottom layers.

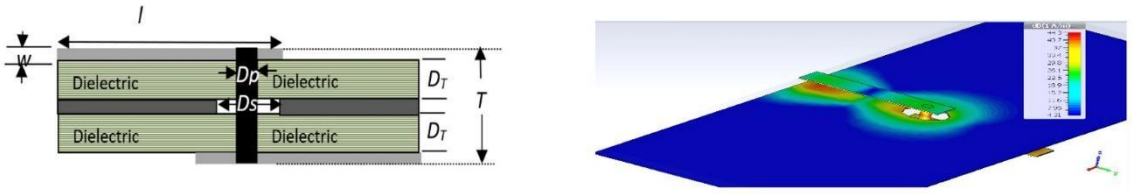

(a) **(b)**

Fig. 3 - Via-hole (a) structure and; (b) current distribution

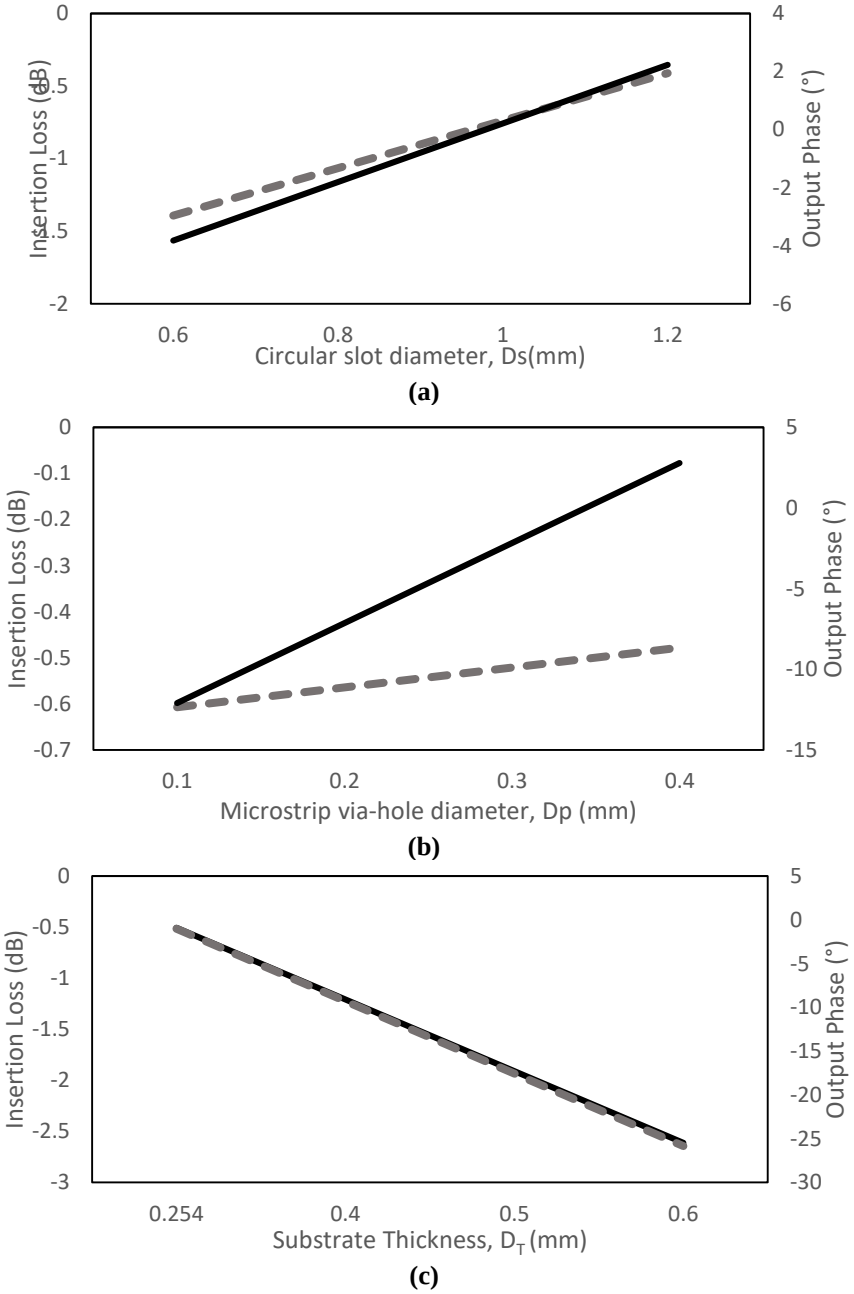

(a)

(b)

(c)

Fig. 4 - Parameter analysis towards the insertion loss (a) circular slot diameter, *Ds* and; (b) via pin diameter, D_P, and; (c) substrate thickness

2.3 Strip Line Analysis

The NPC-F220A substrate, which has a thickness of 0.254 mm, a dielectric constant of 2.2, and a tangent loss of 0.007, is used to determine the strip line characteristics. After considering the impedance of 50 ohms and electrical length of 360 degrees at the operating frequency of 28 GHz, the strip line length, L_0 and W_0, are 7.75 mm and 0.84 mm, respectively. The guided wavelength, λ_g, is 7.2 mm in length and a total length of 360°. Consequently, a 0.02 mm line length results in a 1° phase delay. Phase shift and insertion loss are affected by the additional strip line, ΔL. In this work, the length change, ΔL, is varied from 1 mm to 10 mm, and from the simulation, Fig. 5 shows the insertion loss and phase shift characteristic with 0.029 dB/mm and 47°/mm variations for every strip line dimension, respectively.

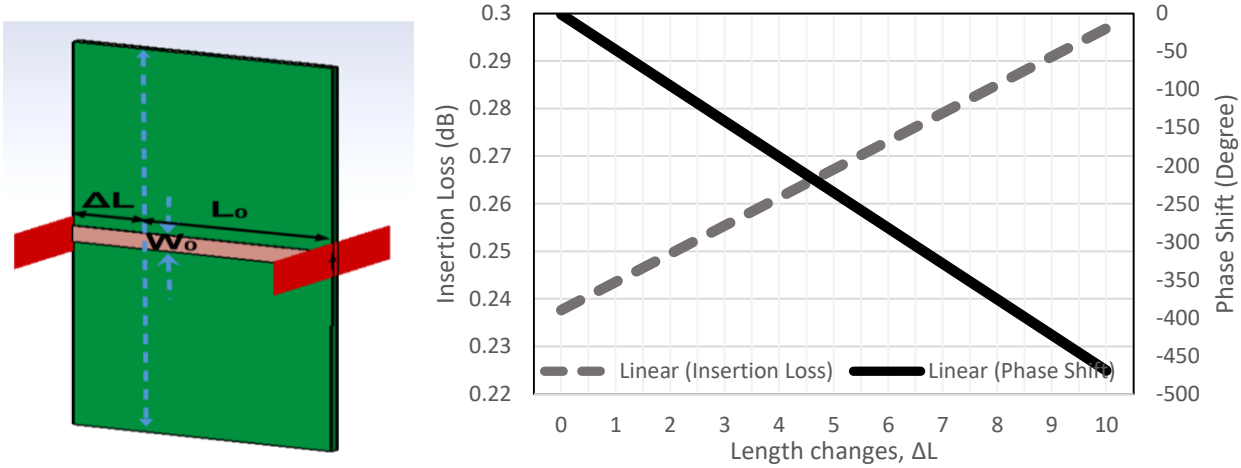

Fig. 5 - Insertion loss and phase shift of the strip line length changes, Δ*L*

2.4 Hybrid

Two transmission lines with λ/4 vertical and horizontal branches connected produce the 3-dB hybrid. The hybrid's horizontal and vertical branches are controlled to determine the output ports' progressive output phase and minimum coupling value. In Fig. 6, a hybrid with four terminal ports is depicted, with the signal becoming transmission when it passes from P1 to P2 and coupling properties when it passes from P1 to P3. The hybrid's dimensions in the proposed design are 3.24 × 6.00 mm^2. The hybrid has values of -29 dB, -3.2 dB, -3.9 dB, -28 dB, and so on for its return loss, S_{11}, insertion loss, S_{21}, coupling, S_{31}, isolation, S_{41}, and output phase difference of 90°.

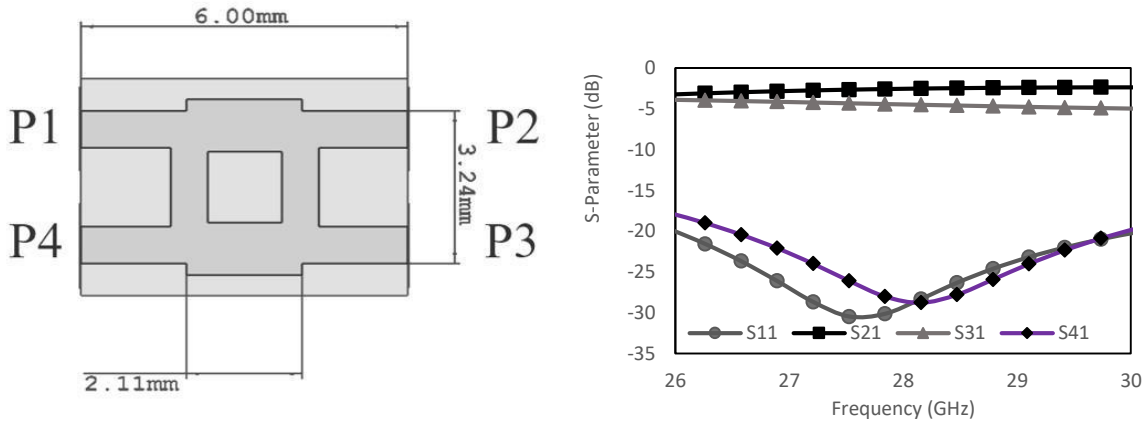

(a) **(b)**

Fig. 6 - Hybrid configuration (a) structure and; (b) S-Parameter

2.5 Butler Matrix with Via-Hole

The Butler Matrix is analyzed using the NPC-F220A substrate. Fig. 7 (a) illustrates the configuration of two hybrids on the upper layer and two hybrids on the lower layer. The hybrids are arranged overlapping between each substrate layer to provide a compact size of BM structure with the overall dimension of 16.47 mm × 7.6 mm. In comparison to [15], the

size reduction is almost 80%. The current distributions through each BM elements are shown in Fig. 7 (b)when one input signal is fed.

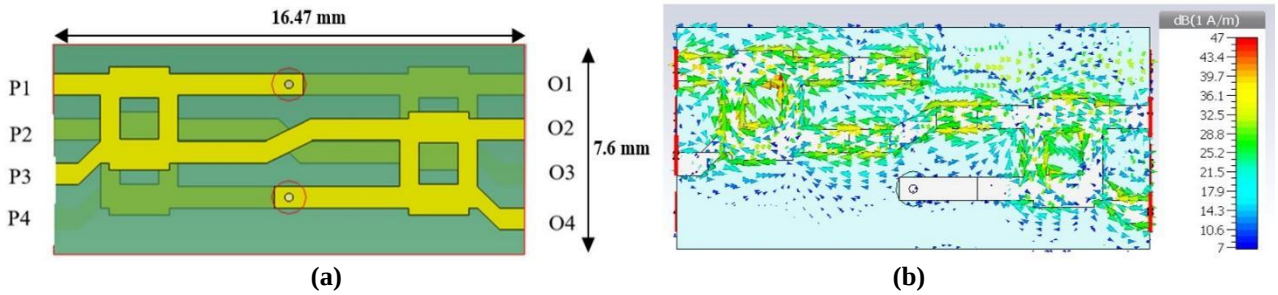

(a) **(b)**

Fig. 7 - Butler Matrix structure (a) side by side and; (b) surface current distribution

2.6 Antenna Array

The directional radiation pattern is formed when the antenna array is arranged at a specified spacing. The array's radiating pattern is controlled by the configuration, the distance between the elements, the amplitude and phase excitation of the elements, and the radiation pattern of individual elements, among other factors. The radiation pattern of the array, excluding the individual element pattern, is used to identify array factors, which can be done by considering the elements as point sources. The array factor can be given as Equation 2 [16]:

$$AF = \sum_{n=1}^{N} e^{+j(n-1)\phi} \tag{2}$$

where $\phi = kd\cos\theta + \beta$

3. Patch Antenna Array Design

An analysis of the rectangular patch antenna and via-hole antenna is discussed in this section. Two types of the patch antenna are used, to construct the patch antenna array. The antenna array is connected to the BM where the performance of the configuration is analyzed.

3.1 Rectangular Patch Antenna

The rectangular patch antenna size is controlled by the substrate's dielectric constant and the resonant frequency. As the operating frequency rises, the patch antenna's size decreases. From Equations 3 to 5, the rectangular patch antenna is designed with a dimension length, L_p, a width, W_p, and a height, h_t, with a substrate thickness of h_s and a permittivity of ε_r. Fig. 8 shows the rectangular patch antenna configuration and the current distributions at 28 GHz. The simulation results for the antenna return loss, S_{11} are < -18 dB. Fig. 9 depicts the antenna's 2D and 3D radiation patterns, respectively where this antenna produces a broadside and symmetric radiation pattern.

Width of rectangular patch antenna, W_p:

$$Wp = \frac{c}{2f_0}\sqrt{\frac{2}{\varepsilon_r + 1}} \tag{3}$$

Effective relative permittivity of substrate, ε_{eff} :

$$\varepsilon_{eff} = \frac{\varepsilon_r + 1}{2} + \frac{\varepsilon_r - 1}{2}\left(1 + 12\frac{h_s}{w_f}\right)^{-0.5} \approx \varepsilon_r \tag{4}$$

Effective length of rectangular patch antenna, L_{eff}:

$$L_{eff} = \frac{c}{2f_0\sqrt{\varepsilon_{eff}}} \tag{5}$$

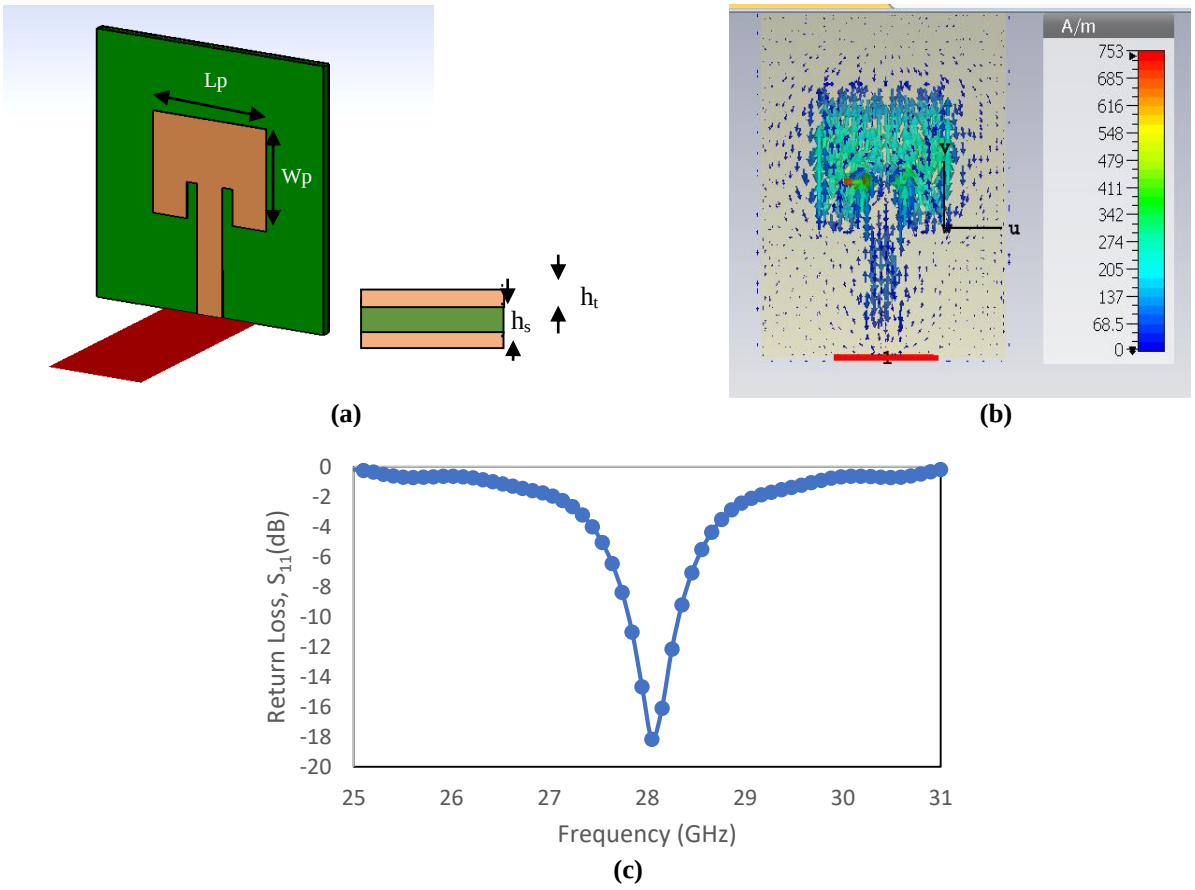

Fig. 8 - Rectangular patch antenna (a) perspective view; (b) surface current distribution and; (c) return loss, S_{11}

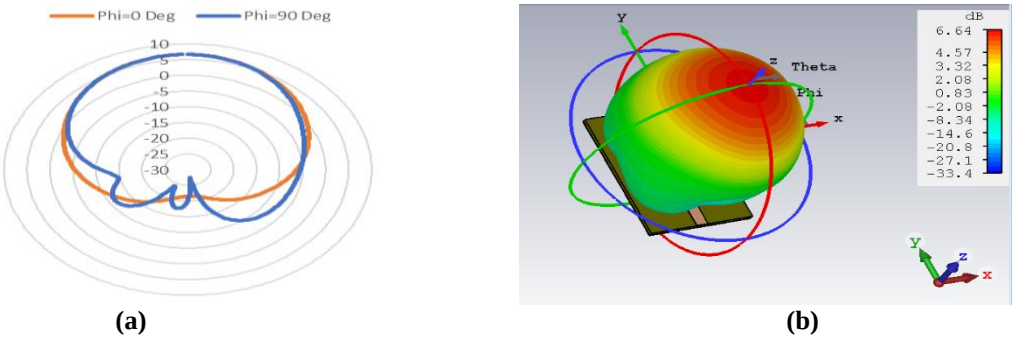

Fig. 9 - Radiation pattern of a rectangular patch antenna (a) 2-D polar and; (b) 3-D polar

3.2 Via-Hole Antenna

The via-hole antenna is designed from a patch that is placed a small fraction of a wavelength above the ground plane and the current distributions are shown in Fig. 10. The feed line is designed at the bottom layer with the ground plane with a circular slot of a diameter of 0.4 mm. The two conducting layers are connected using a via pin with a dimeter of 0.3 mm. The design for a good matching at the design frequency, 28 GHz is obtained from the final position of the via pin is inserted in the point of excitation is 0.68 mm from the lower part of the radiating patch. The return loss performance, S_{11} is less than -20 dB. Fig. 11 depicts the antenna's 2D and 3D radiation patterns, respectively where this antenna produces a broadside and symmetric radiation pattern.

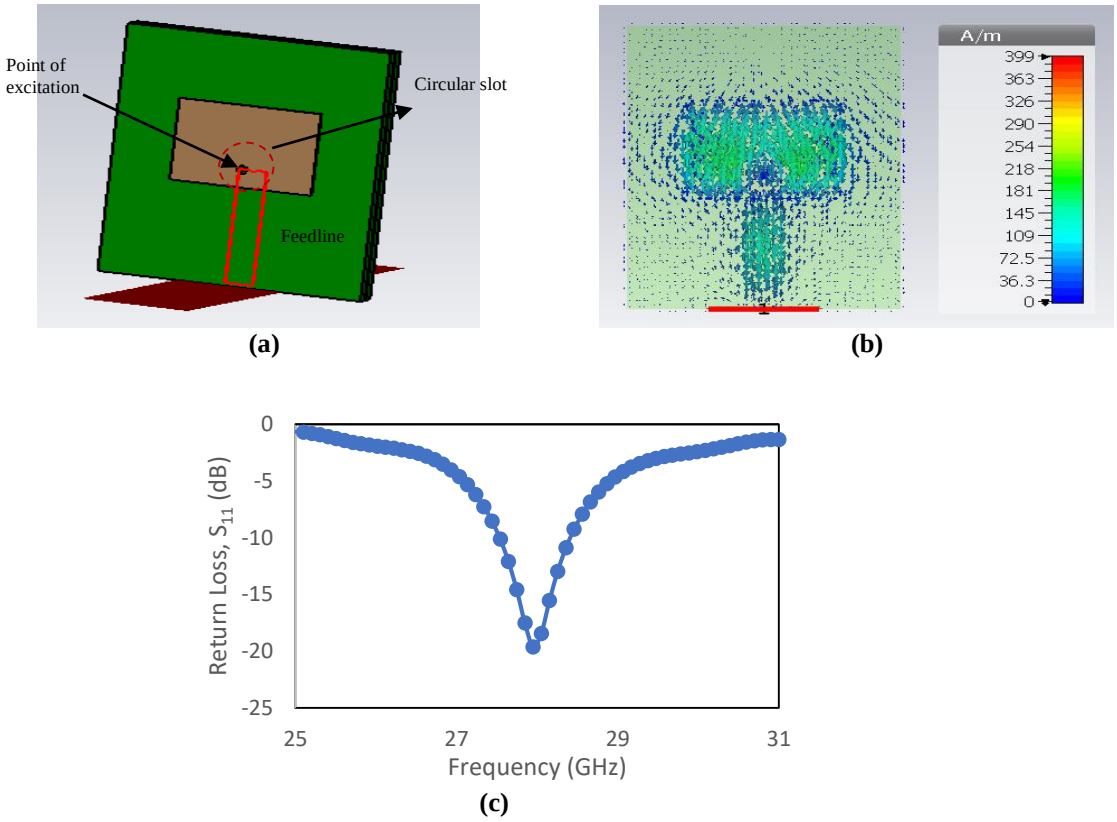

Fig. 10 - Via-hole antenna (a) perspective view; (b) surface current distribution and; (c) return loss, S_{11}

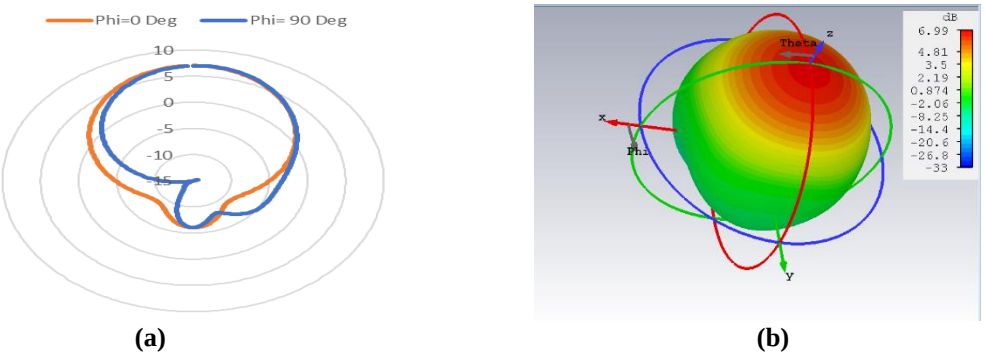

Fig. 11 - Radiation pattern of a via-hole patch antenna (a) 2-D polar and; (b) 3-D polar

3.3 Antenna Patch with Ideal Phase Excitation

The rectangular patch antenna and the via-hole antenna are positioned to be $\lambda_0/2$ between elements as shown in Fig. 12. The ideal input phase and amplitude is fed to each of the input ports of the antenna array using the theoretical value from Table 1. The direction of the beam forming is shown respectively in Fig. 13 with the realized gain of 12.4 dBi, 11.2 dBi, 11.6 dBi and 12.6 dBi where the beam direction is towards +13°, -43°, +40° and -15°.

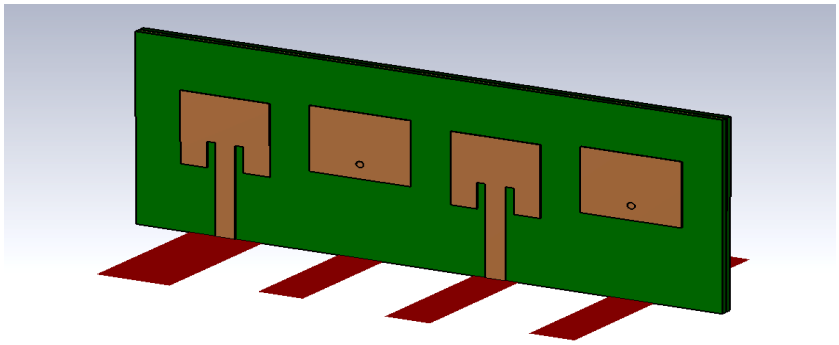

Fig. 12 - Rectangular patch antenna with via-hole patch antenna array with $\lambda_0/2$ spacing

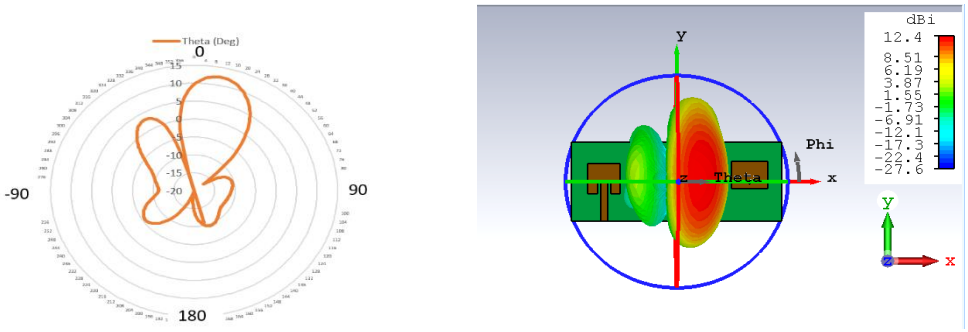

(a)

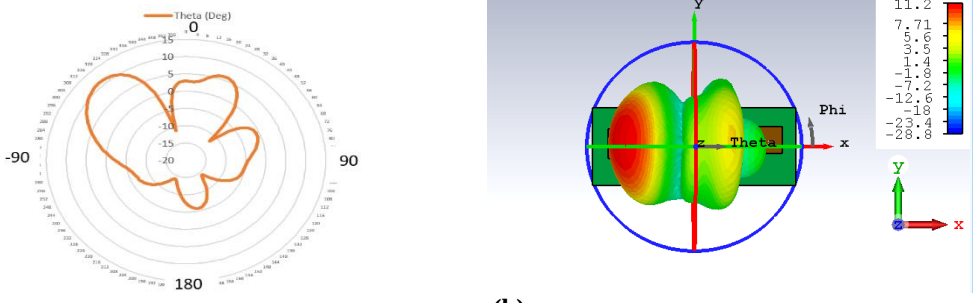

(b)

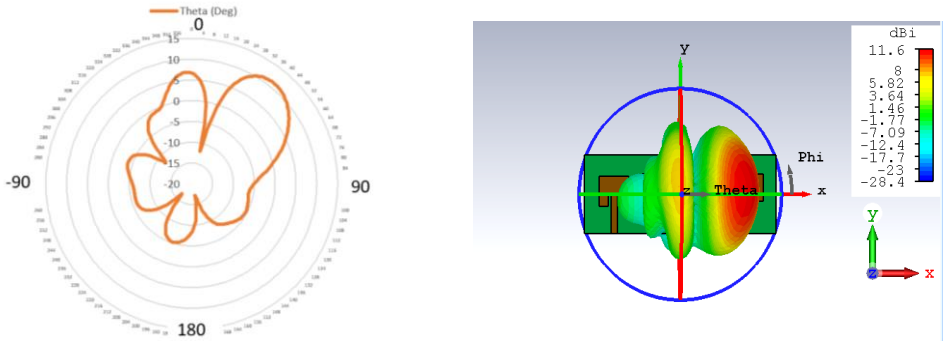

(c)

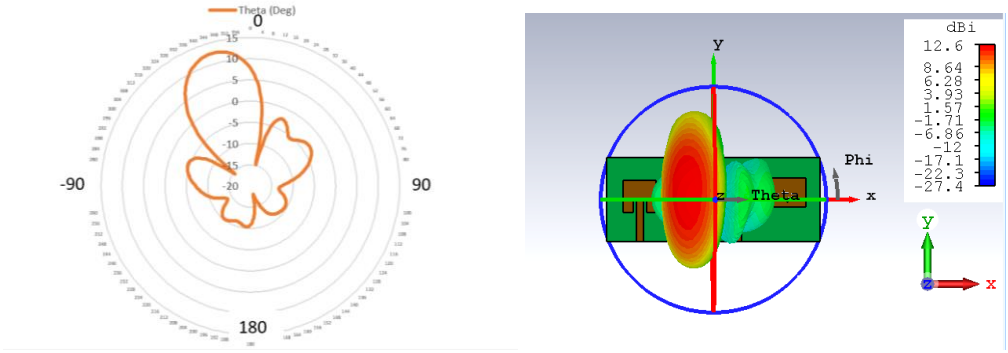

(d)

Fig. 13 - 2 D and 3 D antenna beam direction when signal is fed to (a) port 1; (b) port 2; (c) port 3 and; (d) port 4

3.4 Butler Matrix with Antenna Array Performance

Fig. 14 (a) illustrates the four ports BM with antenna array for the beamforming antenna system. The surface current is illustrated in Fig. 14 (b), where the signal is observed to be distributed through each hybrid, phase shifter and transmission line in the BM. The BM configuration and the antenna array create four beam arrays according to the amplitude and phase output of the BM. The array factor processing creates the four beams based on the phase difference between the output ports.

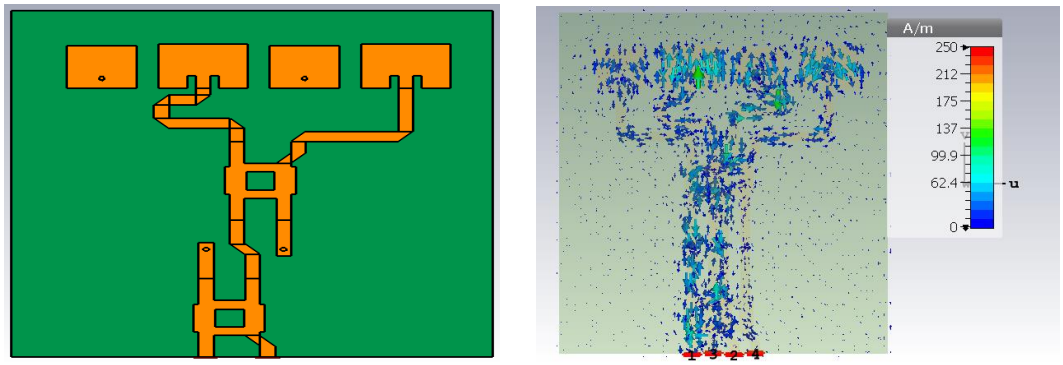

(a) **(b)**

Fig. 14 - Butler Matrix with antenna array (a) configuration and; (b) surface current when input is fed at Port 1

The return loss performance of the input ports (P1-P4) and the output ports (P5-P8) are shown in Fig. 15, with the value is less than -10 dB, which shows small reflection coefficient while the transmission amplitude has the range from -6 ±4 dB at 28 GHz as shown in Fig. 16. In Fig. 17, the phase difference between output ports shows promising results between the theoretical value and the simulation results with small error, ±1° for each of the output phase difference.

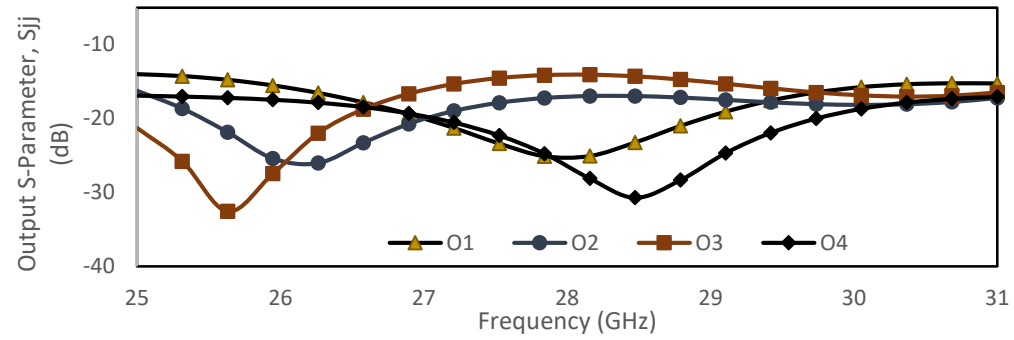

(a)

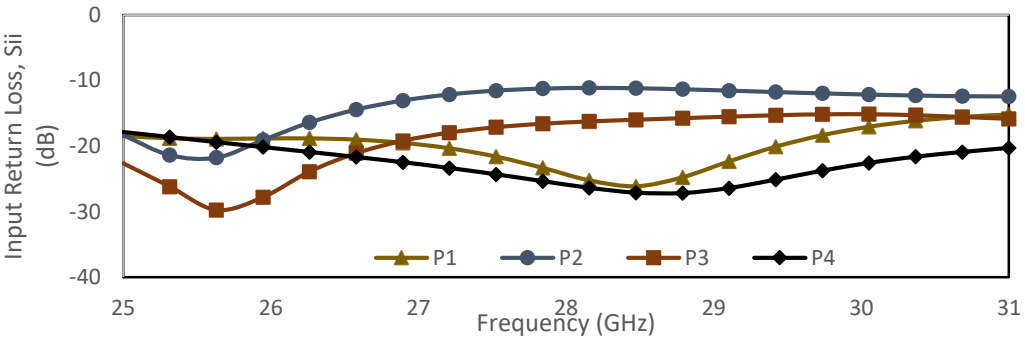

(b)

Fig. 15 - Return loss, S_{ii} at (a) input and; (b) output ports

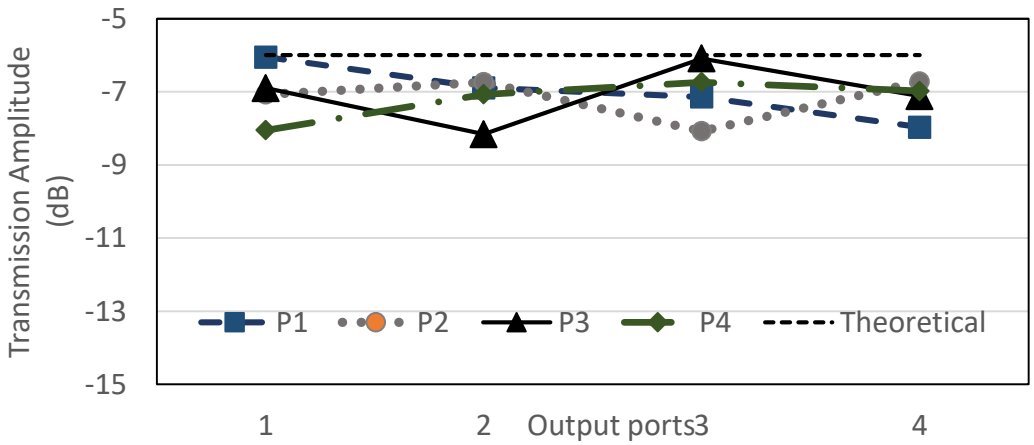

Fig. 16 - Transmission Amplitude, S_{ij} for (a) input P1 (b) input P2 (c) input P3 and (d) input P4

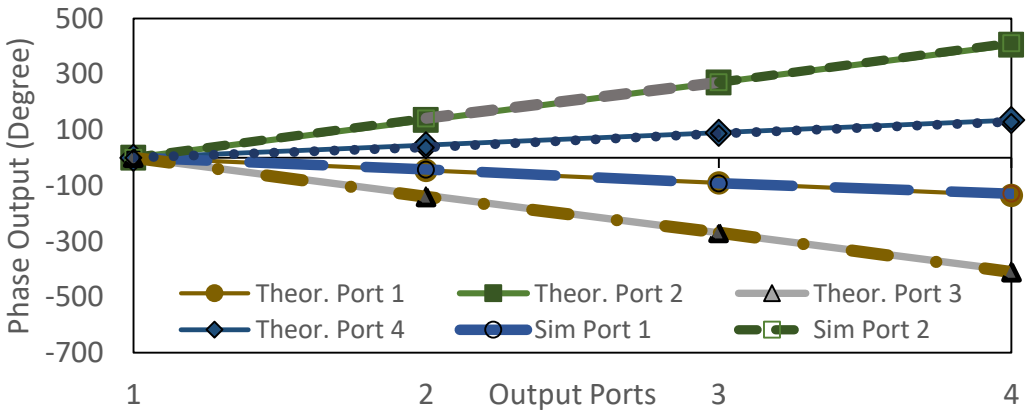

Fig. 17 - Output phase difference of the Butler Matrix

The beam directions of the beamforming antenna system when the four input ports are fed with signals from the BM are shown in Fig. 18. When the Port 1 is fed, the beams radiate in the directions of +16°, -35° when input Port 2 is fed, +39° when input Port 3 is fed, and when the input is fed to Port 4, the beams is pointing to -12°. The gains of each beamforming antenna system are 11.2 dBi, 9.87 dBi, 10.2 dBi, and 11.7 dBi.

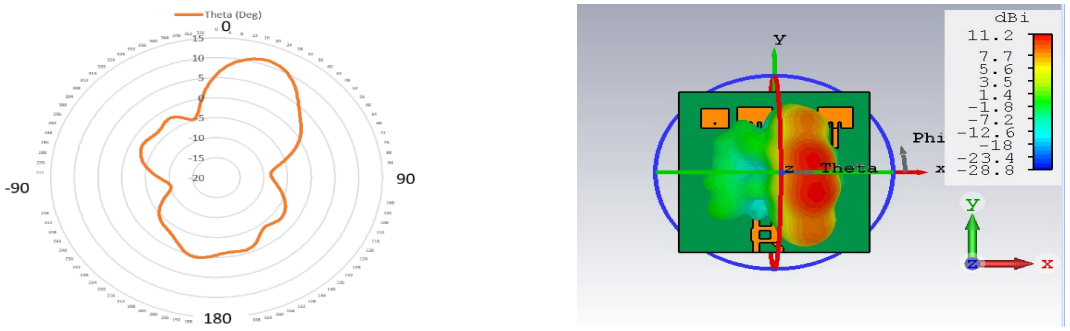

(a)

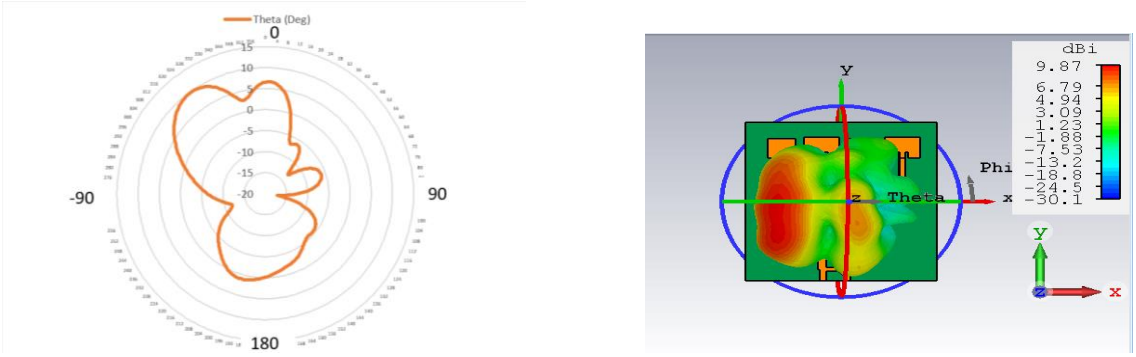

(b)

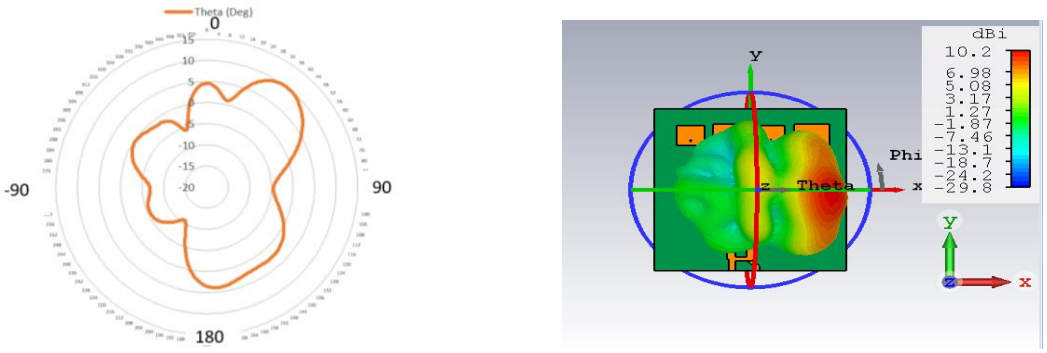

(c)

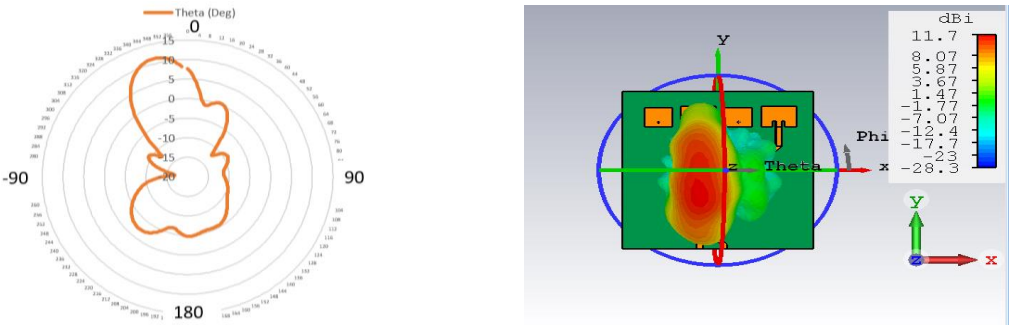

(d)

Fig. 18 - Antenna beam direction when signal is fed to (a) port 1; (b) port 2; (c) port 3 and; (d) port 4

4. Conclusion

In this paper, a via-hole structure BM is designed for the coupling purpose with the via pin is used to connect the two-substrate. The hybrids are connected between two layers by using the via-hole pin and overlapping between each other's, where overall dimension of the BM is compact ($16.47 \times 7.6 \times 0.254$) mm^3 for each substrate. By simplifying the structure and eliminating the crossover elements, this method reduces insertion loss in the structure. In the BM analysis, the transmission coefficient of the output ports has a minimum value of -6 ± 3 dB with a hybrid coupling value of 3 dB. The 4× 4 BM is built of NPC-F220A, a low-loss substrate with a low dielectric constant. At 28 GHz, the return losses and isolation value are both less than 10 dB. When the BM is connected to the antenna array, four beams are produced at +16°, -35°, +39°, and -12°. The four beams are formed with gains of 11.2 dBi, 9.87 dBi, 10.2 dBi, and 11.7 dBi, respectively. The results obtained from the BM simulation is comparable to the ideal phase excitation. The compact size structure can be used to create larger matrix BMs with more input and output ports while maintaining the low loss structure.

Acknowledgement

The authors would like to thank everyone who supported research, especially those from MMU Cyberjaya's Research Management Centre (SAP ID MMUI/220075), Faculty of Engineering, Multimedia University (MMU Cyberjaya), and Communication Systems and Network (CSN i-Kohza), MJIIT, UTM KL.

References

[1] Mahdi, M. N., Ahmad, A. R., Qassim, Q. S., Natiq, H., Subhi, M. A., & Mahmoud, M. (2021). From 5G to 6G Technology: Meets Energy, Internet-of-Things and Machine Learning: A Survey. Appl. Sci, 11, 8117.
[2] Zhang, J., Yu, X., & Letaief, K. B. (2020). Hybrid beamforming for 5G and beyond millimeter-wave Systems: A holistic view. IEEE Open Journal of the Communications Society, 1, 77-91.
[3] Sun, S., Rappaport, T. S., & Shaft, M. (2018). Hybrid beamforming for 5G millimeter-wave multi-cell networks, IEEE INFOCOM 2018 - IEEE Conference on Computer Communications Workshops (INFOCOM WKSHPS), 589-596.
[4] Pozar, D. M. (2011). Microwave Engineering (New York: Wiley).
[5] Tuan, N. T. (2020). Millimeter-Wave Butler Matrix Beamforming Circuit Using Finline in Double-Layer Dielectric Substrate. IEEE Open Journal of Antennas and Propagation, 1, 579-589.
[6] Lee, S., Lee, Y., & Shin, H. (2021). A 28-GHz Switched-Beam Antenna with Integrated Butler Matrix and Switch for 5G Applications. Sensors, 21, 5128.
[7] Qin, C., Chen, F. C., & Xiang, K. R. (2021). A 5 × 8 Butler Matrix Based on Substrate Integrated Waveguide Technology for Millimeter-Wave Multibeam Application. IEEE Antennas Wireless Propag. Lett. 20, 1292-1296.
[8] Zhang, Y., Wu, Y., Wang, W., Yang, Y., & Ma, L. (2021). Novel Multifunctional Dual-Band Coupled-Line Coupler with Reuse of Low-Frequency Trans-Directional and High-Frequency Contra-Directional Functions. IEEE Transactions on Circuits and Systems II: Express Briefs, 68 (6), 1917-1921.
[9] Vallappil, A. K., Rahim, M. K. A., Khawaja, B. A., Murad, N. A., & Mustapha, M. G. (2021). Butler matrix-based beamforming networks for phased array antenna systems: A comprehensive review and future directions for 5G applications. IEEE Access, 9, 3970-3987.
[10] Pezhman, M.M., Heidari, A.A., Ghafoorzadeh-Yazdi, A. (2020). Compact three-beam antenna based on SIW multi-aperture coupler for 5G applications. AEU - International Journal of Electronics and Communications, 123, 153302.
[11] Vahid, R., Ghader, S., Saeid, K., Mesut, K. (2020). Beam-steering high-gain array antenna with FP Bow-tie slot antenna element for pattern stabilisation. IET Microw. Antennas Propag., 14 (11), 1185-1189.
[12] Saeid, K., Vahid, R. (2020). Mutual coupling reduction by SIW ZOR elements on broadside high gain CP beam steering array. Int. J. RF Microw. Comput. Aided Eng., 30 (9), e22286.
[13] Idrus, I.I., Abdul Latef, T., Aridas, N.K., Abu Talip, M.S., Yamada, Y., Abd Rahman, T., Adam, I., Mohd Yasin, M.N. (2019). A low-loss and compact single-layer butler matrix for a 5G base station antenna. PLoS ONE, 14, e0226499.
[14] Moody, H. (1964). The systematic design of the Butler matrix. IEEE Transactions on Antennas and Propagation, 12(6), 786-788.
[15] Md Jizat, N., Yusoff, Z, Mohd Marzuki, A.S., Zainudin, N., Yamada, Y. (2022). Insertion Loss and Phase Compensation Using a Circular Slot Via-Hole in a Compact 5G Millimeter Wave (mmWave) Butler Matrix at 28 GHz. Sensors 22, 5, 1850.
[16] Balanis, C.A. (2005). Antenna Theory Analysis and Design. 3rd Edition, John Wiley & Sons.